Chinese Journal of Oceanology and Limnology
Vol. 35 No. 5, P. 1032-1044, 2017
http://dx.doi.org/10.1007/s00343-017-6037-1

Long-term temperature variation of the Southern Yellow Sea Cold Water Mass from 1976 to 2006*

LI Ang (李昂)[1, 2, 3], YU Fei (于非)[1, **], SI Guangcheng (司广成)[1], WEI Chuanjie (魏传杰)[1]

[1] *Institute of Oceanology, Chinese Academy of Sciences, Qingdao 266071, China*

[2] *University of Chinese Academy of Sciences, Beijing 100049, China*

[3] *Key Laboratory of Research on Marine Hazards Forecasting, National Marine Environmental Forecasting Center, State Oceanic Administration, Beijing 100081, China*

Received Feb. 2, 2016; accepted in principle Apr. 22, 2016; accepted for publication Jul. 31, 2016

Abstract This paper discusses the long-term temperature variation of the Southern Yellow Sea Cold Water Mass (SYSCWM) and examines those factors that influence the SYSCWM, based on hydrographic datasets of the China National Standard Section and the Korea Oceanographic Data Center. Surface air temperature, meridional wind speed, and sea surface temperature data are used to describe the seasonal changes. Mean temperature of the two centers of the SYSCWM had different long-term trends. The temperature of the center in the west of the SYSCWM was rising whereas that of the center in the east was falling. Mean temperature of the western center was related to warm water intrusion of the Yellow Sea Warm Current, the winter meridional wind, and the winter air temperature. Summer process played a primary role in the cooling trend of temperature in the eastern center. A decreasing trend of salinity in the eastern half of the SYSCWM showed that warm water intrusion from the south might weaken, as could the SYSCWM circulation. Weakened circulation provided less horizontal heat input to the eastern half of the SYSCWM. Less lateral heat input may have led to the decreasing trend in temperature of the eastern center of the SYSCWM. Further, warmer sea surface temperatures and less heat input in the deep layers intensified the thermocline of the eastern SYSCWM. A stronger thermocline had less heat flux input from upper layers to this half of the SYSCWM. Stronger thermocline and weakened heat input can be seen as two main causes of the cooling temperature trend of the eastern center of the SYSCWM.

Keyword: Southern Yellow Cold Water Mass (SYSCWM); long-term trend; interannual variability; influence factor

1 INTRODUCTION

The Yellow Sea (YS) is a semi-closed, shallow marginal sea between the Chinese mainland and Korean Peninsula. The YS borders the Bohai Sea to the north and opens to the East China Sea to the south. The Yellow Sea Cold Water Mass (YSCWM) is a significant feature in the YS. The YSCWM occupies a third of the deep part of the YS in summer (Su and Weng, 1994). The YSCWM is a seasonal water mass that is characterized by low temperature and high salinity. It has more conservative characteristics than other water masses in the YS. The region with temperatures below 10°C is seen as the region corresponding to the YSCWM (Su and Weng, 1994). The YSCWM usually has three cold cores (Weng et al., 1988; Tang, 2005) and a strong temperature and salinity front in the YS. The cold core in the northern YS is called the Northern Yellow Sea Cold Water Mass (NYSCWM). The other two cores, in the southern YS, are called the Southern Yellow Sea Cold Water Mass (SYSCWM) (Guo, 1981). The SYSCWM has a large impact on the hydrographic features, biomass, and fishery resources in the YS (Du et al., 1996; Wang et al., 2003; Zhang et al., 2007).

* Supported by the National Natural Science Foundation of China (Nos. 41176018, 41376031, 41206020), the Strategic Priority Research Program of Chinese Academy of Sciences (No. XDA11020301), and the NSFC-Shandong Joint Fund for Marine Science Research Centers (No. U1406401)
** Corresponding author: yuf@qdio.ac.cn

Uda (1934) discovered the existence of the YSCWM in 1934. He et al. (1959) first studied the formation mechanism of the YSCWM and concluded that it was formed locally during the previous winter. Further study by Guan (1963) found that the temperature of the YSCWM had a relationship with local air temperature during the previous winter. Since then, a number of studies on the formation mechanisms of the YSCWM have been published. Formation of the seasonal thermocline (Ren and Zhan, 2005; Yu et al., 2006), surface cooling, strong mixing in winter (Hur et al., 1999), and tidal mixing (Zhao, 1986; Lee and Beardsley, 1999) are all important mechanisms of YSCWM formation.

With the accumulation of historical data, long-term variability of the YSCWM began to draw attention from many academic sectors. Earlier studies explored the distribution range, low temperature center, volume, and thermohaline characteristics of the YSCWM using the similar coefficient method (Weng et al., 1988; Zhang and Yang, 1996). Recent studies on the western half of the SYSCWM have reported that the position and intensity of the thermocline dome and depth have interannual variation (Bai et al., 2004). The temperature at thermocline depth has the greatest temporal variance (Hu and Wang, 2004). Wei et al. (2010) reported that the summer T-S properties of the YSCWM correspond to the Yellow Sea Warm Current (YSWC) in winter. Interannual variability of the eastern half of the SYSCWM has also become of academic interest. Park et al. (2011) conducted Empirical Orthogonal Function (EOF) and Singular Value Decomposition (SVD) analyses using the Korea Oceanographic Data Center (KODC) dataset and described temperature variability of the east SYSCWM. They reported that changes in temperature of the eastern half of the SYSCWM are closely related to changes of atmospheric forcing during summer and winter. Yang et al. (2014) used the same data to show that sea surface temperature (SST) in the previous winter determines the southern edge of the SYSCWM the following summer. SST of the YS has an increasing trend, which is consistent with climate warming in northern China and the adjacent seas (Lin et al., 2005). During the warming season (March to August), the heat content of the upper layer of the YS is primarily owing to shortwave radiation (Wei et al., 2013). Park et al. (2015) examined the relationship between long-term trends of SST and bathymetry and found that the abrupt variation of SST amplitude is related to the Arctic Oscillation signals in winter. An interannual trend of temperature was also seen in some studies of the NYSCWM (Jiang et al., 2007; Li et al., 2015). However, the long-term variation trend of SYSCWM temperature remains unclear, and the influence of summer process is poorly understood. A study on long-term variation of the SYSCWM would be helpful for the interpretation of other variables, such as catches and fishing grounds of demersal fishes (Cho, 1982).

This study aims to identify characteristics of the long-term trend in SYSCWM temperature and to explore the causes of the trend. In Section 2, various datasets used in this study are described. We describe linear trend analysis of the YSCWM temperature and compare the trend difference of the two centers of the SYSCWM in Section 3. In Section 4, we examine the relationship between the bottom temperature and various factors including SST in summer, bottom salinity in June, meridional wind in winter, air temperature in winter, and intrusion of the YSWC. Finally, in Section 5, we summarize the interannual trend properties of SYSCWM temperature and the main factors behind the trend.

2 MATERIAL AND METHOD

2.1 China standard section survey data

These observation data were obtained and archived by the State Oceanic Administration of China. Among the various in situ observation data in the western YS, this dataset has the longest record length and has been used in studies of YSCWM interannual variability (Hu and Wang, 2004; Jiang et al., 2007; Wei et al., 2010). The 36°N standard section temperature data from 1976 to 2006 is used to analyze interannual variability of the western half of the SYSCWM. The measurement precision of temperature data reaches 0.01°C. Ten stations are included in the 36°N section, as shown in Fig.1. The distances of two stations neighboring along the 36°N section are 0.25° near the coast and 0.5° at the central YS. The eastern boundary of this section can reach 124°E. This section covers the western half of the YS; therefore, the data can be used to show the characteristics of the western half of the SYSCWM. Standard levels of the data are 0, 5, 10, 15, 20, 25, 30, 35, 50, and 75 m, plus the bottom depth. Observations in winter and summer were made in February and August, respectively. August data in 1993 are missing and February data are missing in 1976, 1984, and 1996.

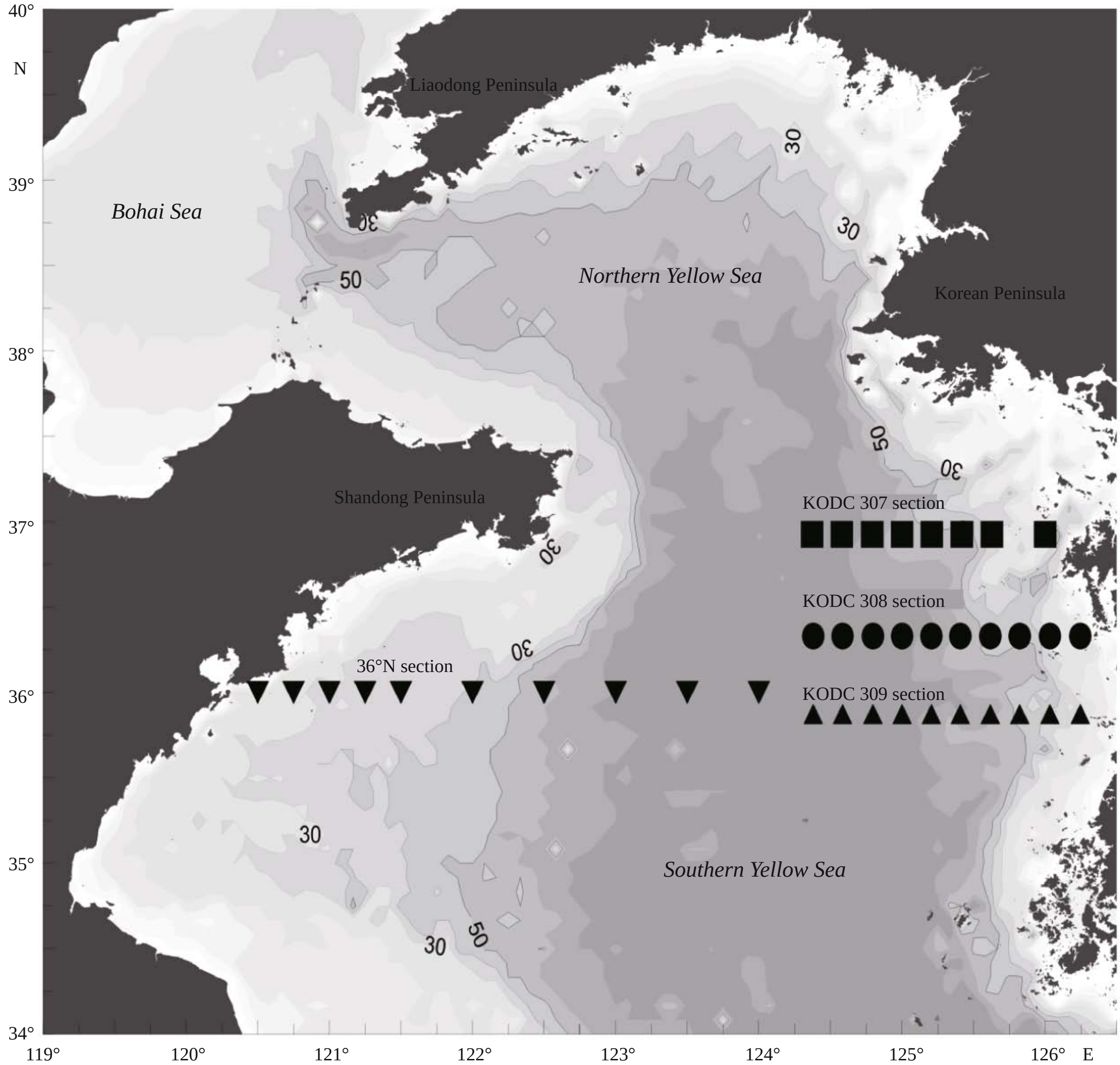

Fig.1 Locations of survey stations: KODC 307 section (squares), KODC 308 section (circles), KODC 309 section (triangles), 36°N section (inverted triangles), and bathymetry (shading)

2.2 Korea Oceanographic Data Center (KODC) data

The KODC dataset is bimonthly observation data that have been routinely collected by the National Fisheries Research & Development Institute of Korea since 1960. The dataset contains various oceanographic parameters, such as temperature, salinity, oxygen, and nutrients. The 307, 308 and 309 section data from 1976 to 2006 are used in this study, and a total of 28 stations are included. These stations stretch across the eastern half of the YSCWM and the west coast of Korea; station locations are shown in Fig.1. The three sections basically cross the eastern half of the SYSCWM from 124.3° to 126.3°E. Zonal spacing of the KODC data is approximately 0.21°, and the meridional distance between two sections is about 0.6°. The vertical levels of the data are 0, 10, 20, 30, 50, and 75 m, plus the bottom depth. The 309 section is at 35.86°N. The latitude difference between the 309 section and 36°N section is only 0.14°; thus, the 309 section can be treated as at the same latitude as the China standard section survey data along 36°N. The summer (winter) observations were made in August (February). The observed time of this dataset shows good consistency.

2.3 ERA-Interim reanalysis data

SYSCWM variability may be associated with the surrounding atmospheric and oceanic conditions in summer and winter. We use atmospheric and oceanic data over the entire YS region as the background field data. The monthly mean data of SST, meridional wind speed at 10 m height, and surface air temperature at 2 m height were used to analyze the climate background. The 28 years of data began in 1979. These data are from the ERA-Interim reanalysis dataset of the European Centre for Medium-Range Weather Forecasts (ECMWF). This dataset is an improved version of the ERA-40, in terms of some key aspects. Dee et al. (2011) described the ERA-Interim reanalysis dataset in detail. The horizontal resolution of the data is 0.125°.

2.4 Hybrid Coordinate Ocean Model (HYCOM) reanalysis data

The model of HYCOM reanalysis data used in this paper is configured for the North and Equatorial Pacific region using HYCOM v2.1.16. The computational domain extends from 98°E to 78°W and 20°S to 65.8°N and the computations are carried out on a Mercator grid with 1/12° equatorial resolution (2 294×1 362 grid points, 6.5 km spacing, on average). There are 33 vertical layers. Bathymetry is derived from a quality controlled ETOPO 2.5 dataset. Surface forcing is from a 6-hourly ECMWF operational product. Kelly et al. (2007) described these data in further detail.

2.5 Mean temperature computing method

The mean temperature is calculated using $\overline{T}=\frac{\sum_{j=1}^{m}\sum_{i=1}^{n_j-1}\left(T_{i,j}+T_{i+1,j}\right)/2\times\left(Z_{i+1,j}-Z_{i,j}\right)}{\sum_{j=1}^{m}\left(Z_{n_j,j}-Z_{1,j}\right)}$, where m is the number of stations east of 122.5°E along the 36°N section (west of 125°E along the 309 section), n_j is the number of vertical levels below 30 m at station j, $Z_{i,j}$ is depth at station j of level i, and $T_{i,j}$ is temperature at station j of level i. As described in Sections 2.1 and 2.2, the vertical levels involved in this equation are 30, 35, 50, 75 m, and bottom level.

2.6 Linear trend analysis method

The one variant linear regression analysis is used to analyze the long-term trend in temperature of the SYSCWM. Regarding the time series of the variable x_i, a one variant linear regression relationship is established as below: $\hat{x}=a+bt_i$, where t_i is time, b is the regression trend, and a is the regression constant. The coefficients a, b are calculated by using least square estimation: $\begin{cases} b=\dfrac{\sum_{i=1}^{n}x_i t_i-\dfrac{1}{n}\left(\sum_{i=1}^{n}x_i\right)\left(\sum_{i=1}^{n}t_i\right)}{\sum_{i=1}^{n}t_i^2-\dfrac{1}{n}\left(\sum_{i}^{n}t_i\right)^2} \\ a=\overline{x}-b\overline{t} \end{cases}$, where n is the length of the time series. The correlation coefficient is used to test the significance level and is calculated as:

$$r=\sqrt{\frac{\sum_{i=1}^{n}t_i^2-\frac{1}{n}\left(\sum_{i=1}^{n}t_i\right)^2}{\sum_{i=1}^{n}x_i^2-\frac{1}{n}\left(\sum_{i=1}^{n}x_i\right)^2}}\ .$$

2.7 Geostrophic current computing method

A dynamic height method is used to compute geostrophic current (Chen et al., 2006). This method is suitable for temperature and salinity data taken from only one section. This method is based on geostrophic approximation, hydrostatic approximation, and β approximation. The computational formula is: $v=v_0\frac{g}{f\rho_0}\int_{z_0}^{z}\frac{\partial\rho}{\partial z}dz$, where $\rho=\rho$ (T, S, P) is density, using the UNESCO state equation to compute density; g is gravitational acceleration; $f=2\Omega\sin\theta$ is the Coriolis parameter; Ω is geostrophic angular velocity; θ is latitude at which the data are taken; ρ_0 is mean density; and v_0 is velocity at the reference level (z_0). In this paper, the bottom depth is selected as the reference level and v_0=0.

3 RESULT AND DISCUSSION

3.1 Interannual trend of temperature

The boundary of 309 and 36°N sections is near 124°E, which is at the YS trough, so this boundary could represent that of the eastern and western halves of the southern YS. Because the mean low temperature center can represent characteristics of the SYSCWM center (Fig.2), we selected the mean temperature of the area (below 30 m and east of 122.5°E along the 36°N section) to represent the mean temperature of the western SYSCWM (W-SYSCWM) in summer. Mean temperature of the area below 30 m and west of 125°E of the 309 section was calculated to represent the mean temperature of the eastern SYSCWM (E-SYSCWM). The computing method was introduced in Section 2.4. Mean temperature of the two sections is shown in Fig.3. The Thermocline was above 30 m. This index of mean temperature can show the vertically averaged temperature of the

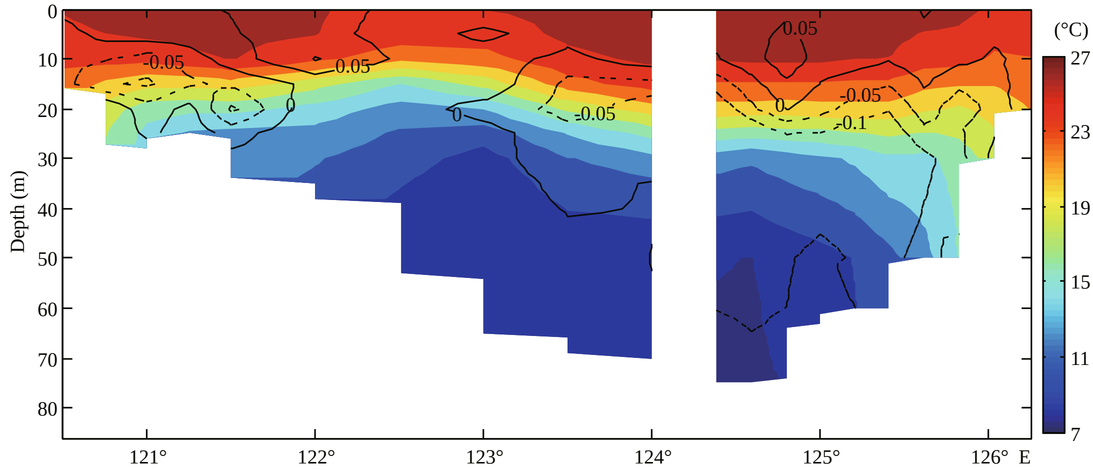

Fig.2 Mean temperature (shading) and linear temperature trend (°C/a, contours), using data from 36°N and 309 sections in August from 1976 to 2006

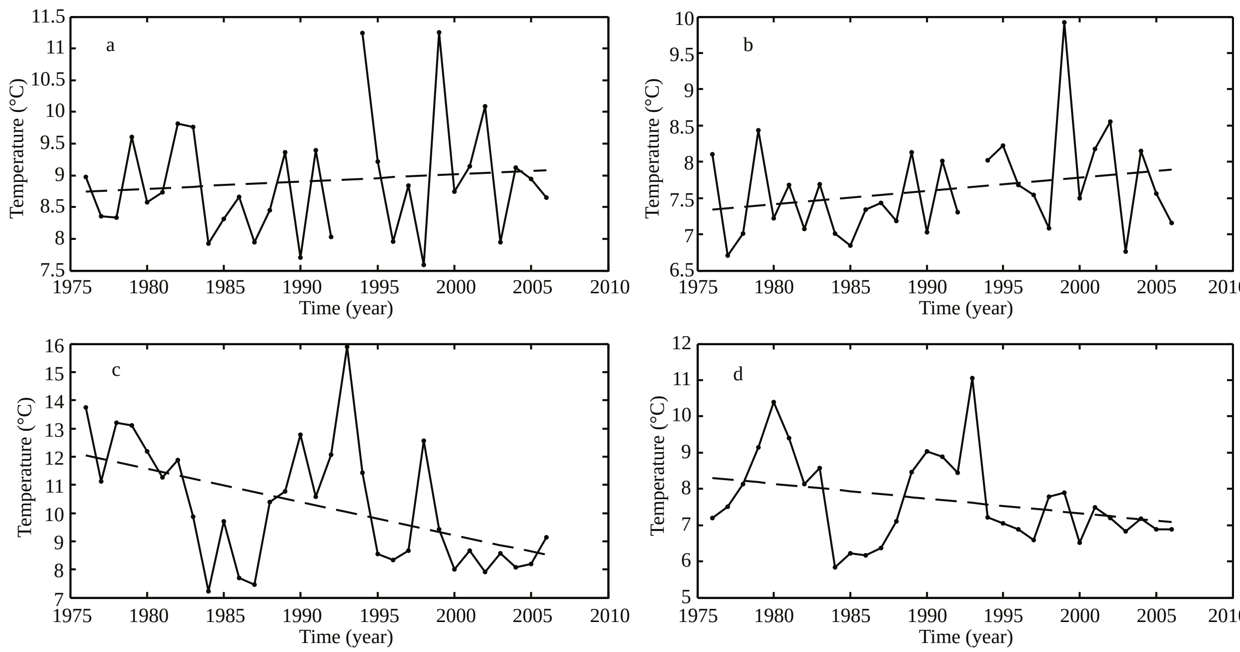

Fig.3 Mean temperature and minimum temperature of W-SYSCWM (a, b) and E-SYSCWM (c, d) in August (solid line) and their linear trends (°C/a, dashed lines)

P-values of Fig.3a, b, c, and d are 0.12, 0.10, 0.08, and 0.01, respectively. Linear correlation coefficients of Fig.3a, b, c, and d are 0.28, 0.31, 0.35, and 0.49, respectively.

SYSCWM area. Variation of the mean temperature of the W-SYSCWM is shown in Fig.3a. The linear trend analysis shows that this temperature had an increasing trend of 0.01°C per year. However, mean temperature of the E-SYSCWM had a different long-term trend (Fig.3c). The range of this temperature was 7.23°C (1984) to 15.89°C (1993), and its mean interannual difference ~1.65°C. The decreasing trend of E-SYSCWM temperature reached 0.12°C per year. The different trends of the two SYSCWM cores are also shown by various temperature indices. The minimum temperature of the 36°N section in summer shows an ascending trend (Fig.3b), at 0.02°C per year. This trend is similar to that of mean temperature of the W-SYSCWM. Minimum temperature of the E-SYSCWM had a decreasing trend (Fig.3d), at -0.04°C per year. This shows the same trend as that of mean temperature of the E-SYSCWM. Park et al. (2015) indicated that some areas had a cooling trend at 30 and 50 m. The minimum temperatures also indicate that temperatures of the W-SYSCWM and E-SYSCWM had different trends.

To further study the different temperature trends of the western and eastern SYSCWM, linear trends of

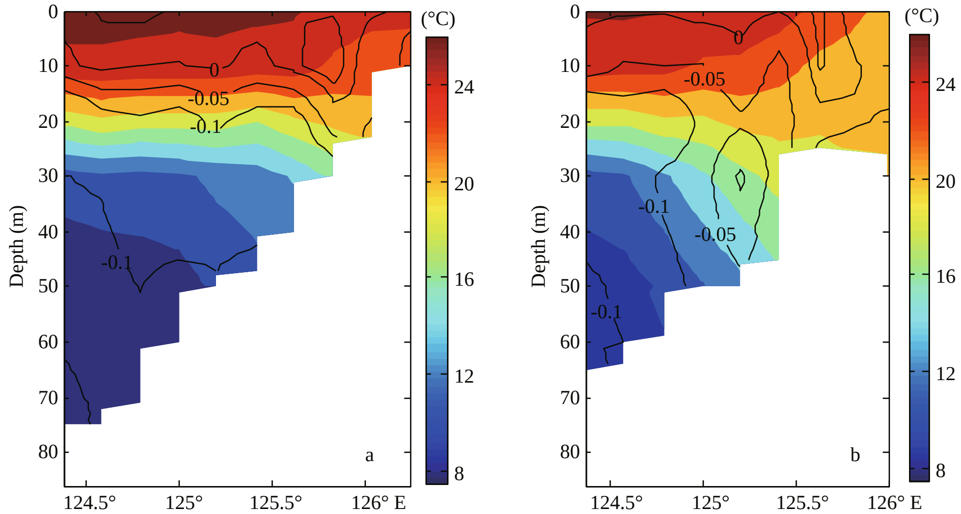

Fig.4 Mean temperature (shading) and linear temperature trend (°C/a, contours) of 308 section (a) and 307 section (b) in August from 1976 to 2006

time series of the 36°N and 309 section data were calculated (Fig.2, solid contours). Under the background of global warming, SSTs of the two sections showed rising trends. The temperature trend from 10 to 30 m may be related to interannual variation of the thermocline (Hu and Wang, 2004). In the deep layers, temperatures of the two sections had different interannual trends. The decreasing trend exceeded 0.1°C per year at some stations along the 309 section. Similar temperature trends were found on the 307 and 308 sections (Fig.4). Both of the maximum temperature decreasing trends of the two sections exceeded 0.1°C per year. These interannual variations are consistent with the mean temperature trend of E-SYSCWM, which was described earlier. Analysis of all section data indicates opposite long-term trends between the two cold cores of the SYSCWM.

In this section, temperature indices of the SYSCWM were examined, such as the mean value of the low temperature center and minimum temperature. Trends of W-SYSCWM and E-SYSCWM were confirmed. Temperature of the W-SYSCWM had an increasing trend while that of the E-SYSCWM had a decreasing trend. Factors that caused this difference are explored in subsequent sections.

3.2 Factors influencing W-SYSCWM temperature

3.2.1 Variation of winter temperature

The local water mass in winter is a significant source of the YSCWM (He et al., 1959). Therefore, the temperature of the YS in winter is important to variability of the SYSCWM temperature in summer. We calculated linear trends and mean temperatures using the 36°N and 309 section temperature data in February to represent winter temperature conditions (Fig.5). Owing to the influences of strong mixing and low air temperature, winter temperature of the YS was nearly homogenous in the upper and lower layers. All temperature data show increasing trends, so the winter YS temperature rose. We selected mean temperature below 30 m of the 36°N and 309 sections in winter to investigate mean temperatures in the eastern and western YS. This area was the same as that in summer. The YSWC is a major source of heat flux input and warm water to the YS. Though the intrusion of the YSWC had a clear westward shift along the western slope of the YS trough, the high-temperature input of the YSWC could affect temperature of the entire YS. These mean values of deep-layer temperature along the 36°N and 309 sections revealed the intrusion of the YSWC into the western and eastern SYSCWM to some degree. The heat flux input brought by the YSWC is seen as a major influence on SYSCWM temperature. The warming trend of the YS in winter shows that the source of the SYSCWM had a warming trend. The difference between W-SYSCWM temperatures in summer and winter was smaller than the difference between E-SYSCWM temperatures in those seasons (Fig.6). The correlation coefficient of the two indices was 0.40, with confidence coefficients >90%. Mean temperature of the W-SYSCWM in winter increased by 0.03°C per year. This indicates that the warm water brought in by the YSWC had an increasing trend. The W-SYSCWM shows strongly conservative properties. The higher temperature of warm water increased the winter YS temperature.

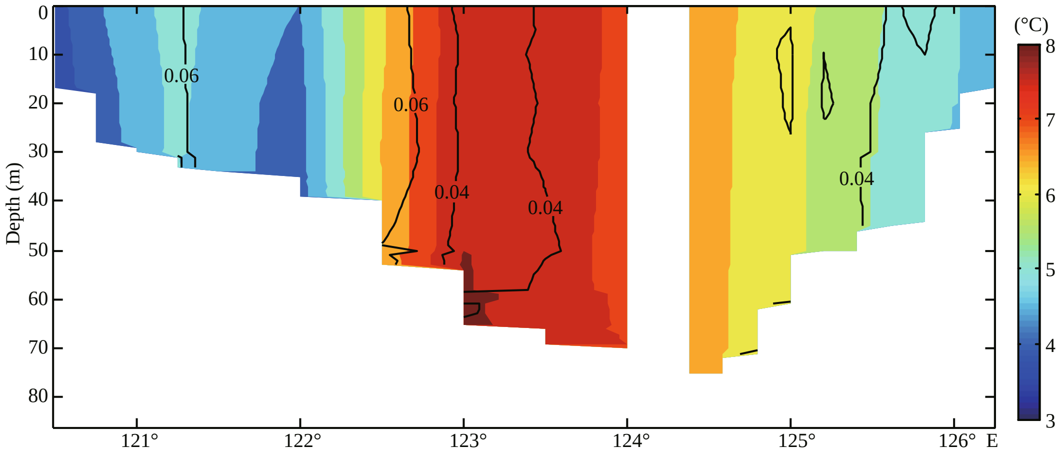

Fig.5 Mean temperature (shading) and linear temperature trend (°C/a, contours), using data from 36°N and 309 sections in February from 1976 to 2006

3.2.2 Variation of winter forcing factors

Winter climatic elements such as local wind and air temperature are important factors that can affect the temperature of the YS. We calculated the area-average meridional wind speed from December to February in the YS (119°–124°E, 35°–37°N) to describe winter monsoon conditions there. The correlation coefficient between that wind and mean temperature of the W-SYSCWM is 0.41 (Fig.7a). This indicates that the stronger the northerly wind was, the lower the temperature of the W-SYSCWM. Northerly winds in winter advects cold air and induces stronger vertical mixing. A strong winter monsoon can affect the interannual variability of W-SYSCWM temperature.

Air temperature is also an important winter forcing factor. The area-average air temperature was calculated to portray the temperature pattern in winter. The same area and time used for the meridional wind speed were used for temperature. Air temperature in winter has a close relationship with the SYSCWM. The correlation coefficient between air temperature in winter and mean temperature of the W-SYSCWM is 0.38 (Fig.7b), at a significance level of 90%. Under the background of global warming, the temperature had an increasing trend of 0.03°C per year. The *P*-value and *R*-squared values of linear regression at a significance level of 90% were 0.06 and 0.13, respectively. A warmer air temperature in winter produces a higher temperature of the W-SYSCWM in summer.

Correlation analysis showed that the local winter climate factors affect the strength of the W-SYSCWM. Further, the air temperature in winter had an increasing trend. The atmospheric and oceanic elements in that season tended to raise the temperature of the W-SYSCWM.

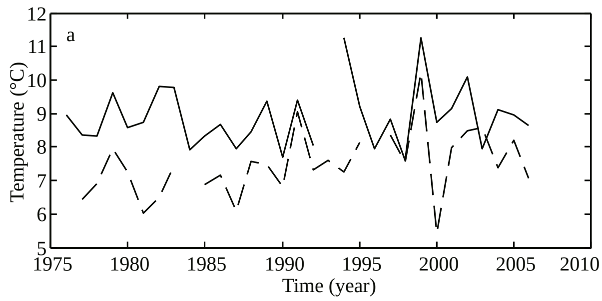

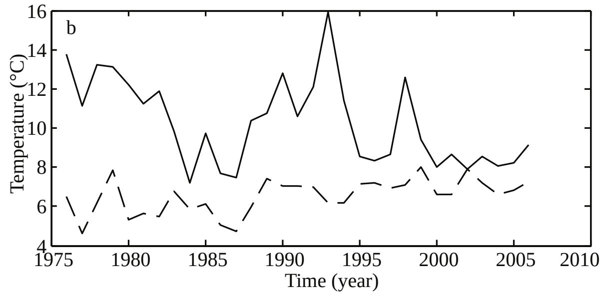

Fig.6 Mean temperature of W-SYSCWM in August (solid curve) and February (dashed curve) from 36°N section (a); mean temperature of E-SYSCWM in August (solid curve) and February (dashed curve) from 309 section (b)

3.3 Factors influencing E-SYSCWM temperature

In contrast with the above, in the eastern half of the YS, the correlation analysis showed that the mean temperature of the same area as the E-SYSCWM in winter had no obvious correlation with E-SYSCWM temperature in summer (Fig.6b). The correlation coefficient was only -0.03 and the correlation did not pass the 90% confidence test. The bottom temperature in the eastern YS changed more than that in the western YS from winter to summer. Although the strength of the YSWC in winter can influence the temperature there by modifying the heat flux into the

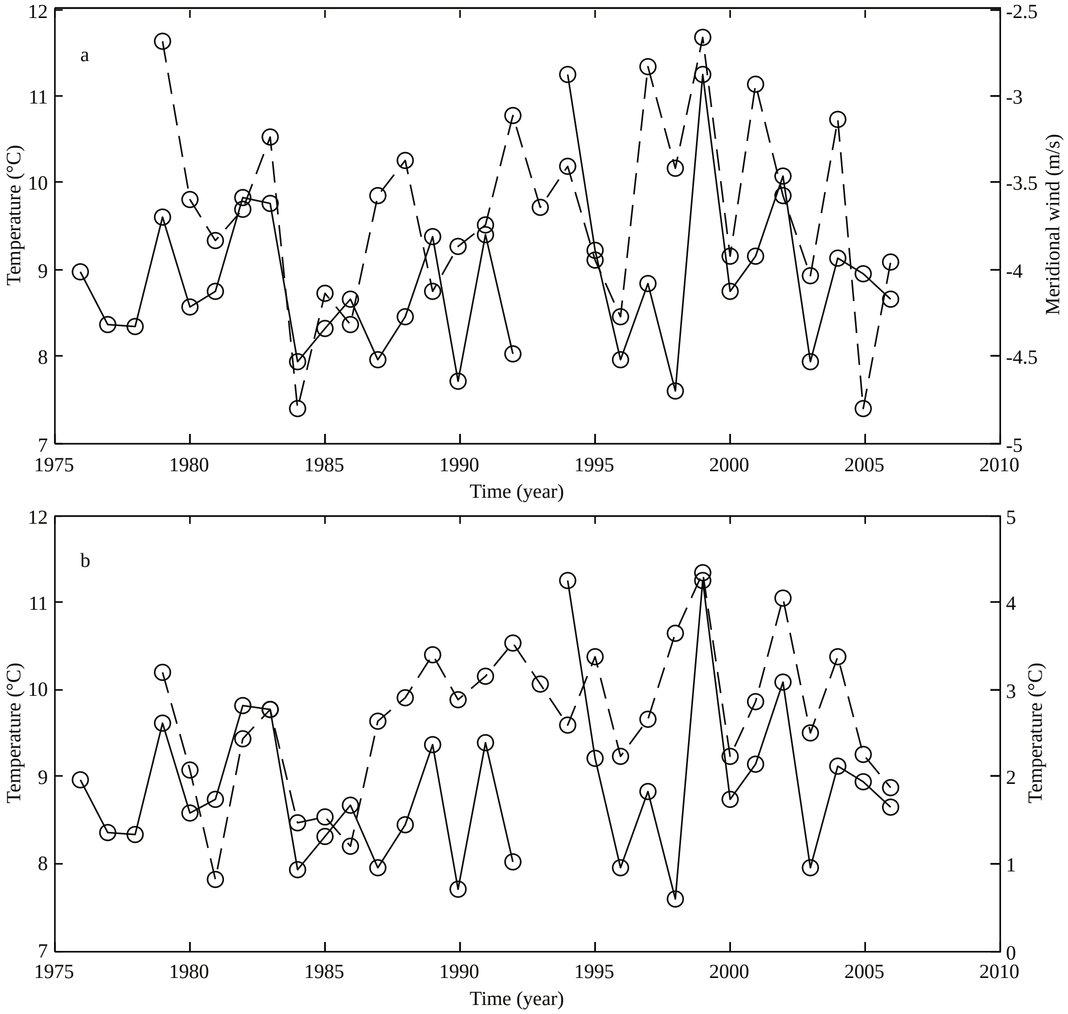

Fig.7 Mean temperature of W-SYSCWM in August (solid curve) and mean meridional wind (dashed curve) of YS in winter from 36°N section (a); mean temperature of W-SYSCWM in August (solid curve) and mean air temperature (dashed curve) of YS in winter from 36°N section (b)

southern YS the previous winter, the warming trend of water temperature in winter was not the reason for the cooling trend of the E-SYSCWM.

3.3.1 Variation of summer process

The water temperature and climatic elements of the YS in winter cannot be used to explain the temperature trend of the E-SYSCWM. It may be spring or summer processes that induced the trend in Fig.2c. We calculated mean temperature of the E-SYSCWM using data from the 309 section in April and June. The computation and area used for April and June data were the same as those for August data. Mean temperature of the E-SYSCWM showed an increase from April to August in most years. The difference of mean temperature of the E-SYSCWM between June and August was greater than that between April and June (Fig.8b). Temperatures of the entire 309 section in April still showed a warming trend (Fig.9a). In June, a cooling trend began to appear in the thermocline and coastal area (Fig.9b). The cooling trend of the E-SYSCWM may form and develop from June to August, and the summer process may have a primary role in the decreasing trend of temperature of that water mass.

3.3.2 Circulation of YS during summer

Horizontal heat transport is an important modifier of the thermal structure of the SYSCWM in summer. The flow field can change horizontal heat input to the SYSCWM. In both observational (Beardsley et al., 1992; Tang et al., 2000; Pang et al., 2004) and numerical studies (Yanagi and Takahashi, 1993; Xia et al., 2006; Moon et al., 2009), the upper-layer (4–40 m) cyclonic circulation of the YS has been revealed. The model result of meridional current in

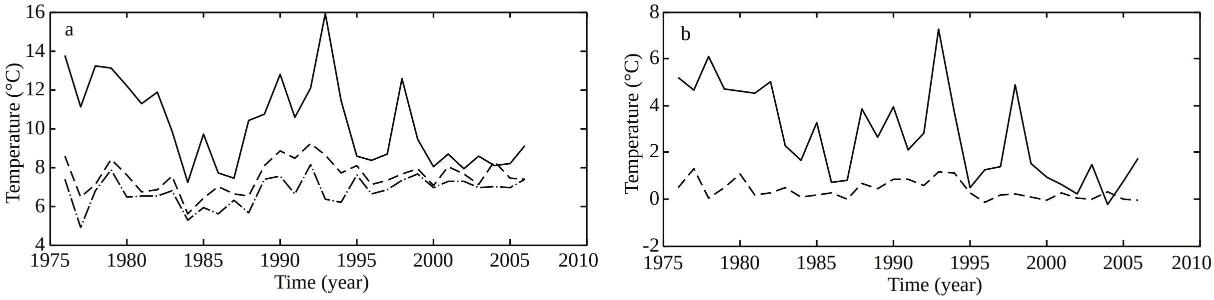

Fig.8 Mean temperature of E-SYSCWM in August (solid curve), June (dashed curve), and April (dot-dashed curve) (a); difference between mean temperature of E-SYSCWM in August and that in June (solid curve), and difference between mean temperature of E-SYSCWM in June and that in April (dashed curve) (b)

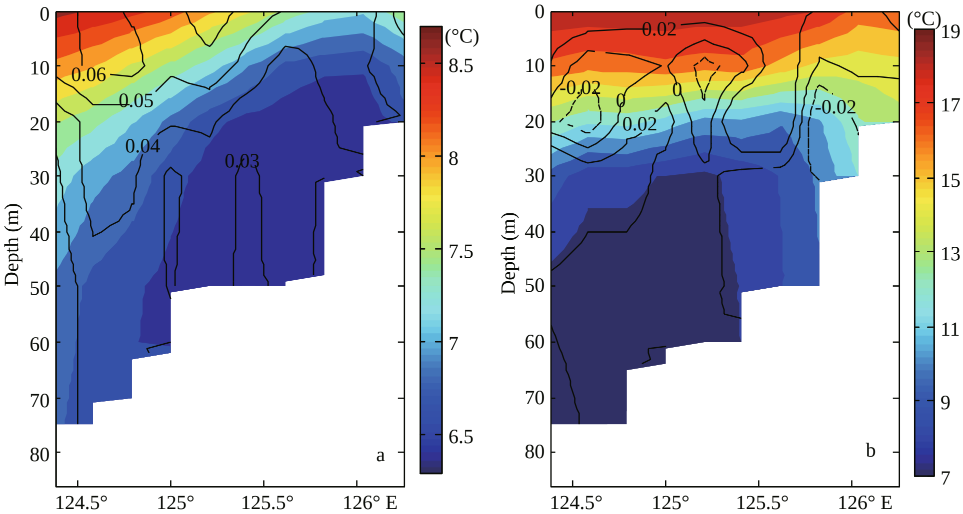

Fig.9 Mean temperature (shading) and linear temperature trend (°C/a, contours) of 309 section in April (a) and June (b) from 1976 to 2006

Fig.10 is similar to the geostrophic current obtained using the dynamic height method (Fig.11). The mean geostrophic current in summer shows that the dominant flow was southward in the western half of the YS and northward in the eastern half. The northward flow brings in more warm water from the southern part of the YS. This raises the temperature of the E-SYSCWM. Though tidal residual currents contribute to the formation of southward flow in the bottom layer (Xia et al., 2006), tidal component M_2 (the only tidal component included in Xia's simulation) had very little interannual variability. Thus, the tidal residual current may have no obvious effect on interannual variation of southward flow in the bottom layer. In addition, tidal residual current data are difficult to obtain. Therefore, we only considered interannual variation of the YS circulation in summer. Warm water from the southern YS increases the temperature of the E-SYSCWM in summer.

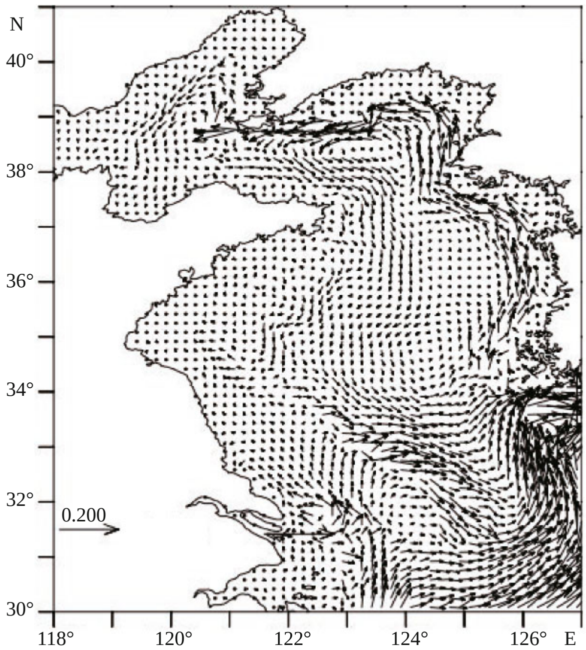

Fig.10 Simulated flow field at depth 10 m in August, in m/s (Xia et al., 2006)

The YSCWM is also more saline than the coastal

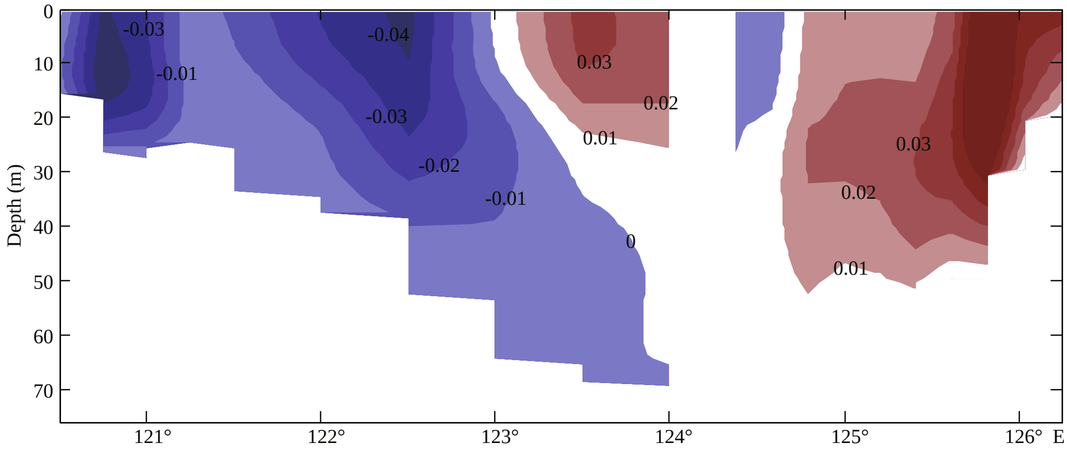

Fig.11 Averaged geostrophic current speed (m/s), using data from 36°N and 309 sections in August during 1976–2006

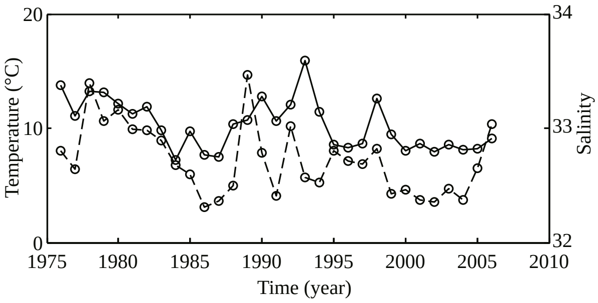

Fig.12 Mean temperature of E-SYSCWM in August (solid curve) and mean salinity of E-SYSCWM in June (dashed curve)

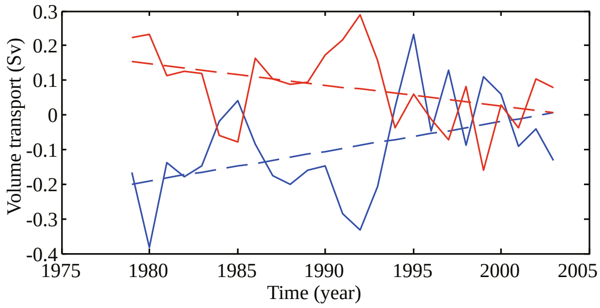

Fig.13 Mean volume transport of W-SYSCWM area from June to August (blue solid curve) and its trend (blue dashed curve); mean volume transport of E-SYSCWM area from June to August (red solid curve) and its trend (red dashed curve)

water mass. Changes in salinity can have diverse causes such as precipitation, oceanic currents, and river discharge. The impact of precipitation is mainly on the surface layer, whereas the E-YSCWM is in the deep layer (below 30 m) of the eastern YS. The E-YSCWM area is west of 125°E and far from the estuaries of Korea's Han and Changjiang Rivers. Further, the vertical diffusion coefficient of salinity is less than that of temperature. Therefore, advection caused by oceanic currents from the southern YS may be the main influence on the mean salinity of the E-YSCWM area. The high-salinity tongue may be seen as an intrusion of warm water. This can somewhat reveal the local current field. The mean E-SYSCWM salinity based on the 309 section in June was decreasing (Fig.12). The computation and area of mean salinity were the same as those of the E-SYSCWM mean temperature. The range of the decreasing trend was 0.015 per year. This shows that the warm and saline water transport in the E-SYSCWM during June may be weakened. The correlation analysis showed the average high-salinity center of the eastern YS in June was related to the mean temperature of the E-SYSCWM. The correlation coefficient reached 0.5. Less warm water intrusion slows the warming of the E-SYSCWM in summer.

Using HYCOM reanalysis data of 36°N, mean volume transport from June through August in the area 124.3°–125°E and 30–50 m was calculated to represent volume transport of the E-SYSCWM area in summer; that of the area 122.5°–124°E and 30–50 m represents volume transport of the W-SYSCWM area in summer. Volume transports of the E-SYSCWM and W-SYSCWM areas had opposite phase tendencies. Linear trends of volume transport of the E-SYSCWM and W-SYSCWM areas were -0.006 Sv/a and -0.01 Sv/a, relatively. Transport of the E-SYSCWM area was negative, which means that the northward current weakened. Transport of the W-SYSCWM area was positive, which means that the southward current weakened. The weakening trend of meridional current shows that the SYSCWM circulation may have weakened. The correlation coefficient of volume transport of the two areas was -0.78 (Fig.13), at a 95% significance level. Further, the correlation analysis showed that the average

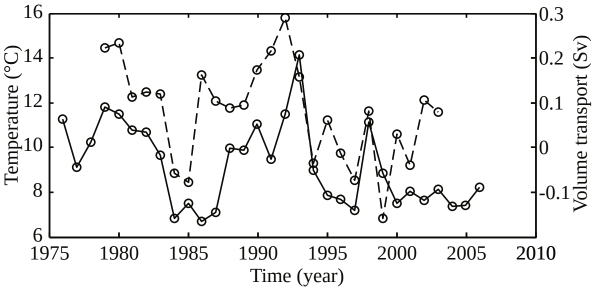

Fig.14 Mean temperature of E-SYSCWM in August (solid curve) and mean volume transport of E-SYSCWM area from June to August (dashed curve)

volume transport of the E-SYSCWM area from June to August was related to the E-SYSCWM mean temperature (Fig.14). The correlation coefficient was 0.6, at a 95% significance level. Further, volume transport of the E-SYSCWM area had a decreasing trend, at -0.01 Sv/a. The decreasing volume transport reduced horizontal heat input. The decrease of volume transport of the E-SYSCWM area weakens the warming of the E-SYSCWM.

The reduced horizontal volume transport may be caused by a weakened circulation of the YS in summer. Such weaker circulation brings less cold water to the W-SYSCWM, warming it. The weaker circulation of the SYSCWM also brings less warm water to the E-SYSCWM. The decline of lateral heat input weakens the warming of the E-SYSCWM from June to August. As a result, the E-SYSCWM temperature did not rise as much as before and so its temperature became relatively low.

3.3.3 Thermocline variation during summer

The thermocline can affect YSCWM formation (Ren and Zhan, 2005). It can also inhibit vertical thermal mixing. We calculated the mean SST above the E-SYSCWM along the 309 section in June to describe summer SST in the area (Fig.15a). This SST was increasing at the rate of 0.04°C per year, and its correlation coefficient with average E-SYSCWM temperature was -0.56. Lateral heat input in the bottom layer weakened. The increasing trend of SST and less warm-water intrusion intensified the thermocline. Further, we calculated the vertical temperature gradient along the 309 section in June. The maximum vertical gradient above the E-SYSCWM is regarded as thermocline strength (Fig.15b). The range of thermocline strength was from 0.49°C/m (1976) to 1.19°C/m (1984). The mean interannual difference of thermocline strength was about 0.18°C/m. The strength in June also had a

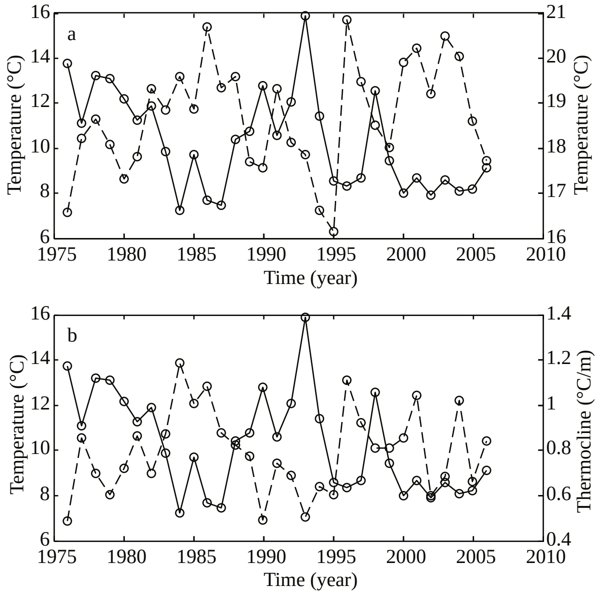

Fig.15 Mean temperature of E-SYSCWM in August (solid curve) and mean SST in June (dashed curve) (a); mean temperature of E-SYSCWM in August (solid curve) and maximum vertical temperature gradient in June (dashed curve) (b)

relationship with mean temperature of the E-SYSCWM. The correlation coefficient was -0.64. Thermocline strength also had a slight increasing trend (0.002°C/m/a). A stronger thermocline generates less vertical heat exchange across it.

Less warm-water intrusion reduces the horizontal heat input. This could result from the weakening of the YS circulation in summer. Increasing SST and less bottom-layer horizontal heat input enhanced the temperature difference between the surface and bottom layer. The stronger thermocline inhibited vertical heat exchange, thereby weakening E-SYSCWM warming from June to August. The increasing SST of the YS and less warm-water intrusion may be the main causes of the E-SYSCWM cooling trend.

4 CONCLUSION

We identified characteristics of long-term trends of the SYSCWM and examined causes of those trends. We used the KODC, China Standard Section, and ERA-interim datasets.

Temperatures in the eastern and western SYSCWM showed different interannual trends. The mean W-SYSCWM temperature had an increasing trend, while that of the E-SYSCWM had a decreasing trend. Minimum temperature in the two regions of the YS had the same trends as the mean temperatures. The linear trend analysis of 36°N, 307, 308 and 309 section data supported that temperatures in the eastern and western SYSCWM had opposite long-term trends.

In winter, temperatures of the 36°N and 309 sections became warmer. The average temperature of that area in winter showed a positive correlation with W-SYSCWM temperature in summer. As the source of the SYSCWM, the warming trend of local water in winter indicates the reason why the W-SYSCWM became warmer. However, the temperature of the eastern YS in winter had no obvious relationship with E-SYSCWM temperature. The warming of local water did not cool E-SYSCWM water.

Further, winter factors such as mean meridional wind and air temperature had strong impacts on temperature variability of the W-SYSCWM. The mean meridional wind speed over the YS was positively correlated with W-SYSCWM temperature, with a correlation coefficient of 0.41. Surface air temperature in winter had a similar positive correlation with W-SYSCWM (0.38). Air temperature in winter had a warming trend. Higher temperatures heated the local water and increased W-SYSCWM temperature.

Summer processes were primary in the E-SYSCWM cooling trend. The warming range of the E-SYSCWM from June to August was greater than that from April to June. The E-SYSCWM warming from June to August was more obvious.

Decreasing heat input in the deep layer and a strengthening thermocline were two important factors for the declining trend of E-SYSCWM temperature. A stronger thermocline and less lateral heat transport weakened vertical and horizontal heat fluxes into the E-SYSCWM, respectively. A decreasing trend of E-SYSCWM salinity in June indicated that warm-water transport might have been weakened. Weakened heat input inhibited E-SYSCWM warming from June to August. The reduced warm-water intrusion in summer might have been caused by the weakened circulation of the YS in summer. Further, SST of the eastern YS showed a long-term increasing trend. The warming trend of SST and less horizontal heat input sharpened the thermocline. The stronger thermocline reduced heat exchange between the upper and bottom layers. Accordingly, warming of the E-SYSCWM in summer weakened, and this caused relatively cold temperatures in the E-SYSCWM.

5 ACKNOWLEDGMENT

We are grateful to reviewers for their helpful comments. The KODC data can be downloaded at http://kodc.nfrdi.re.kr. The ERA-Interim reanalysis data can be downloaded from http://apps.ecmwf.int/datasets/data/interim-full-moda/. The HYCOM reanalysis data can be downloaded at http://hycom.org/.

References

Bai H, Hu D X, Chen Y L, Wang Q Y. 2004. Statistic characteristics of thermal structure in the southern Yellow Sea in summer. *Chinese Journal of Oceanology and Limnology*, **22**(3): 237-243, http://dx.doi.org/10.1007/BF02842554.

Beardsley R C, Limeburner R, Kim K, Candela J. 1992. Lagrangian flow observations in the East China, Yellow and Japan seas. *La Mer*, **30**(3): 297-314.

Chen H X, Yuan Y L, Hua F. 2006. Multi-core structure of the main part of the Kuroshio at G-PN section in the East China Sea. *Chinese Science Bulletin*, **51**(6): 738-746, http://dx.doi.org/10.1007/s11434-006-0738-8.

Cho K D. 1982. On the influence of the Yellow Sea bottom cold water on the demersal fishing grounds. *Bulletin of the Korean Fisheries Technology Society*, **18**(1): 25-33.

Dee D P, Uppala S M, Simmons A J, Berrisford P, Poli P, Kobayashi S, Andrae U, Balmaseda M A, Balsamo G, Bauer P, Bechtold P, Beljaars A C M, Van De Berg L, Bidlot J, Bormann N, Delsol C, Dragani R, Fuentes M, Geer A J, Haimberger L, Healy S B, Hersbach H, Hólm E V, Isaksen L, Kållberg P, Köhler M, Matricardi M, McNally A P, Monge-Sanz B M, Morcrette J J, Park B K, Peubey C, De Rosnay P, Tavolato C, Thépaut J N, Vitart F. 2011. The ERA-Interim reanalysis: configuration and performance of the data assimilation system. *Quarterly Journal of the Royal Meteorological Society*, **137**(656): 553-597.

Du B, Zhang Y J, Shan Y C, Wang H. 1996. The characteristics of Cold Water Mass variation at the bottom of the north Yellow Sea and its hydrological effects on the mortality of shellfish cultured in the waters of outer Chang-Shan Island. *Marine Science Bulleten*, **15**(4): 17-28. (in Chinese with English abstract)

Guan B X. 1963. A preliminary study of the temperature variations and the characteristics of the circulation of the Cold Water Mass of the Yellow Sea. *Oceanologia et Limnologia Sinica*, **5**(4): 255-284. (in Chinese with English abstract)

Guo B L. 1981. The temperature and salinity structures and the circulation in the Yellow Sea. *In*: Proceedings of Japan-China ocean Study Symposium on Physical Oceanography and Marine Engineering in the East China Sea. Shimizu. p.174-197.

He C B, Wang Y X, Lei Z Y, Xu S. 1959. A preliminary study of the formation of Yellow Sea cold mass and its properties. *Oceanologia et Limnologia Sinica*, **2**(1): 11-15. (in Chinese with English abstract)

Hu D X, Wang Q Y. 2004. Interannual variability of the southern Yellow Sea cold water mass. *Chinese Journal of*

Oceanology and Limnology, **22**(3): 231-236, http://dx.doi.org/10.1007/BF02842553.

Hur H B, Jacobs G A, Teague W J. 1999. Monthly variations of water masses in the Yellow and East China Seas, November 6, 1998. *Journal of Oceanography*, **55**(2): 171-184, http://dx.doi.org/10.1023/A:1007885828278.

Jiang B J, Bao X W, Wu D X, Xu J P. 2007. Interannual variation of temperature and salinity of northern Huanghai Sea Cold Water Mass and its probable cause. *Acta Oceanologica Sinica*, **29**(4): 1-10, http://dx.doi.org/10.3321/j.issn:0253-4193.2007.04.001. (in Chinese with English abstract)

Kelly K A, Thompson L, Cheng W, Metzger E J. 2007. Evaluation of HYCOM in the Kuroshio Extension region using new metrics. *Journal of Geophysical Research*: *Oceans*, **112**(C1): C01004, http://dx.doi.org/10.1029/2006JC003614.

Lee S H, Beardsley R C. 1999. Influence of stratification on residual tidal currents in the Yellow Sea. *Journal of Geophysical Research*: *Oceans* (*1978-2012*), **104**(C7): 15 679-15 701, http://dx.doi.org/10.1029/1999JC900108.

Li A, Yu F, Diao X Y, Si G C. 2015. Interannual variability of temperature of the northern Yellow Sea Cold Water Mass. *Acta Oceanologica Sinica*, **37**(1): 30-42, http://dx.doi.org/10.3969/j.issn.0253-4193.2015.01.004. (in Chinese with English abstract)

Lin C L, Ning X R, Su J L, Lin Y A, Xu B. 2005. Environmental changes and the responses of the ecosystems of the Yellow Sea during 1976-2000. *Journal of Marine Systems*, **55**(3-4): 223-234, http://dx.doi.org/10.1016/j.jmarsys.2004.08.001.

Moon J H, Hirose N, Yoon J H. 2009. Comparison of wind and tidal contributions to seasonal circulation of the Yellow Sea. *Journal of Geophysical Research*: *Oceans*(*1978-2012*), **114**(C8), http://dx.doi.org/10.1029/2009JC005314.

Pang C G, Liang J X, Hu D X, Wang F, Chen Y L, Bai H, Bai X Z. 2004. Surface circulation patterns observed by drifters in the Yellow Sea in summer of 2001, 2002 and 2003. *Chinese Journal of Oceanology and Limnology*, **22**(3): 209-216, http://dx.doi.org/10.1007/BF02842550.

Park K A, Lee E Y, Chang E, Hong S. 2015. Spatial and temporal variability of sea surface temperature and warming trends in the Yellow Sea. *Journal of Marine Systems*, **143**: 24-38.

Park S, Chu P C, Lee J H. 2011. Interannual-to-interdecadal variability of the Yellow Sea Cold Water Mass in 1967-2008: characteristics and seasonal forcings. *Journal of Marine Systems*, **87**(3-4): 177-193, http://dx.doi.org/10.1016/j.jmarsys.2011.03.012.

Ren H J, Zhan J M. 2005. A numerical study on the seasonal variability of the Yellow Sea cold water mass and the related dynamics. *Journal of Hydrodynamics*, **20**(S): 887-896, http://dx.doi.org/10.3969/j.issn.1000-4874.2005.z1.012. (in Chinese with English abstract)

Su Y S, Weng X C. 1994. Water masses in China seas. *In*: Zhou D, liang Y B, Zeng C K C K T eds. Oceanology of China Seas. Kluwer Academic Publishers, The Netherlands. p.3-16.

Tang Y X, Zou E M, Lie H J, Lie J H. 2000. Some features of circulation in the southern Huanghai Sea. *Acta Oceanologica Sinica*, **22**(1): 1-16. (in Chinese with English abstract)

Tang Y. 2005. Yellow Sea Cold Water Mass. *In*: Su J ed. Hydrography of China Offshore. Ocean Press, China. p.202-206. (in Chinese)

Uda M. 1934. Hydrographical research on the normal monthly conditions in the Japan Sea, the Yellow Sea, and the Okhotsk Sea. *J*. *Imp*. *Fish*. *Exp*. *Stn*., **5**: 191-236.

Wang R, Zuo T, Wang K. 2003. The Yellow Sea cold bottom water—an oversummering site for *Calanus sinicus* (Copepoda, Crustacea). *Journal of Plankton Research*, **25**(2): 169-183, http://dx.doi.org/10.1093/plankt/25.2.169.

Wei H, Shi J, Lu Y Y, Peng Y. 2010. Interannual and long-term hydrographic changes in the Yellow Sea during 1977-1998. *Deep Sea Research Part II*: *Topical Studies in Oceanography*, **57**(11-12): 1 025-1 034, http://dx.doi.org/10.1016/j.dsr2.2010.02.004.

Wei H, Yuan C Y, Lu Y Y, Zhang Z H, Luo X F. 2013. Forcing mechanisms of heat content variations in the Yellow Sea. *Journal of Geophysical Research*: *Oceans*, **118**(9): 4 504-4 513, http://dx.doi.org/10.1002/jgrc.20326.

Weng X C, Zhang Y K, Wang C M, Zhang Q L. 1988. The Variational characteristics of the Huanghai Sea (Yellow Sea) Cold Water Mass. *Oceanologia et Limnologia Sinica*, **19**(4): 368-379. (in Chinese with English abstract)

Xia C S, Qiao F L, Yang Y Z, Ma J, Yuan Y L. 2006. Three-dimensional structure of the summertime circulation in the Yellow Sea from a wave-tide-circulation coupled model. *Journal of Geophysical Research*: *Oceans* (*1978-2012*), **111**(C11), http://dx.doi.org/10.1029/2005JC003218.

Yanagi T, Takahashi S. 1993. Seasonal variation of circulations in the East China Sea and the Yellow Sea. *Journal of Oceanography*, **49**(5): 503-520.

Yang H W, Cho Y K, Seo G H, You S H, Seo J W. 2014. Interannual variation of the southern limit in the Yellow Sea Bottom Cold Water and its causes. *Journal of Marine Systems*, **139**: 119-127, http://dx.doi.org/10.1016/j.jmarsys.2014.05.007.

Yu F, Zhang Z X, Diao X Y, Gou J S, Tang Y X. 2006. Analysis of evolution of the Huanghai Sea Cold Water Mass and its relationship with adjacent water masses. *Acta Oceanologica Sinica*, **28**(5): 26-34, http://dx.doi.org/10.3321/j.issn:0253-4193.2006.05.003. (in Chinese with English abstract)

Zhang G T, Sun S, Yang B. 2007. Summer reproduction of the planktonic copepod *Calanus sinicus* in the Yellow Sea: influences of high surface temperature and cold bottom water. *Journal of Plankton Research*, **29**(2): 179-186, http://dx.doi.org/10.1093/plankt/fbm005.

Zhang Y K, Yang Y L. 1996. Analyses of the variational characteristics of the north Huanghai Sea Cold Water Mass. *Marine Forecasts*, **13**(4): 15-21. (in Chinese with English abstract)

Zhao B R. 1986. The fronts of the Huanghai cold water mass (HCWM) induced by tidal mixing. *Chinese Journal of Oceanology and Limnology*, **4**(2): 159-170, http://dx.doi.org/10.1007/BF02850432.